DOI https: //doi. org/10.1007/s11595-020-2363-9

Improved Removal Efficiency of Submicron Inclusions in Non-oriented Silicon Steel during RH Process

CHEN Tianying, JIN Yan, CHENG Zhaoyang, YUAN Zexi, BI Yunjie, LIU Jing
(The State Key Laboratory of Refractories and Metallurgy, Wuhan University of Science and Technology, Wuhan 430081, China)

Abstract: To improve the removal efficiency of such submicron inclusions, we designed an argon blowing method for an RH facility based on mathematical simulations. The effect of the argon blowing on the liquid steel flow and the movement of submicron inclusions was studied using the k-ε flow model coupled with the DPM model for inclusion movement based on fluid computational dynamics in FLUENT. It was found that a more uniform argon flow can be achieved in the up-leg snorkel with a new nozzle position and inner diameter, which resulted in a favorable up-lifting and mixing movement. The new design also increased the circulation rate of molten steel in the RH chamber. The increased turbulent kinetic energy and turbulent dispersing rate enhanced the collision probability of submicron inclusions, which results in an improved removal for 0.5-1 μm inclusions. The proposed RH facility could increase the removal rate of submicron inclusions from the original 57.1% to 66.4%, which improves the magnetic properties of non-oriented silicon steel.

Key words: RH treatment; argon blowing method; model optimization; submicron inclusions; numerical simulation

1 Introduction

Non-oriented silicon steel has been widely used in high-efficiency motors due to its excellent magnetic properties due to a low iron loss and a high magnetic induction strength[1]. However, the presence of inclusions in non-oriented silicon steel has detrimental effects on its magnetic properties, particularly the presence of submicron inclusions[2-4].

Modern steelmaking utilizes RH (Ruhrstahl Heraeus) refining to improve the purity of silicon steels. However, RH-treated silicon steels still contain a large range of inclusions, with more than 35% being submicron inclusions[5]. The removal efficiency of submicron inclusions during the RH process depends primarily on the flow behavior.

As the reaction in a RH vessel is complex, mathematical models[6-8] have been developed to study the flow and inclusion collision behavior during treatment to better understand the flow dynamics. One of the key factors that determine the efficiency and effectiveness of vacuum refining is the Ar nozzles. In general, an increased number of Ar nozzles will improve the efficiency of circulation because of the greater amount of up-lifting gas bubbles[9]. However, too many nozzles in the upper-leg will adversely impact the performance of the refractory lining; therefore, the optimum number of nozzles in most RH degassers is between 4 and 8, depending on the actual working conditions. Research has shown that reducing the inner diameters of the Ar nozzles allows the bubbles to develop a more uniform leading[10]. This results in an increased up-lifting efficiency despite the volume reduction of the gas bubbles. In addition, smaller gas bubbles are favorable for the removal of submicron inclusions. Ai[11] established a removal model for alumina inclusions in RH refining and found that the removal rate increased with the particle size only for large inclusions (>50 μm), but little difference was seen for the removal rates of 2-50 μm inclusions.

Submicron inclusions in non-oriented silicon steels have strong detrimental effects on its magnetic properties by inhibiting grain growth and pinning the domain wall movement. However, there is limited research that simulates the movement of submicron inclusions in such steels. In this work, numerical models were used to calculate the effects of Ar nozzles on the

(Received: Oct. 19, 2019; Accepted: Feb. 20, 2020)

CHEN Tianying(陈天颖): E-mail: chentianying@yeah.net.
*Corresponding author: LIU Jing(刘静): Prof.;E-mail: liujing@wust.edu.cn

Funded by the National Natural Science Foundation of China (No. 51804231) and the Key R&D Program of Hubei Province (No. 2020BAA027)

flow field and the removal rate of submicron inclusions in non-oriented silicon steel during RH treatment. In combination with previous experimental data[5], we propose a new Ar nozzle design to achieve an improved removal efficiency.

In addition, the conservation equations for the number and mass of inclusions during the growth process can be expressed as:

$$\frac{\partial}{\partial t}(\rho N^*)+\nabla\left[\rho\left\{\frac{4}{9\sqrt[3]{36}}\cdot\frac{g}{\rho_1 v_1}\cdot(\rho_1-\rho_g)\cdot r^{*2}+u_1\right\}N^*\right] = \nabla\cdot(D_{\text{eff}}\nabla N^*)+S_{N^*} \quad (1)$$

$$\frac{\partial}{\partial t}(\rho C^*)+\nabla\left[\rho\left\{\frac{4}{9\sqrt[3]{36}}\cdot\frac{g}{\rho_1 v_1}\cdot(\rho_1-\rho_g)\cdot r^{*2}+u_1\right\}C^*\right] = \nabla\cdot(D_{\text{eff}}\nabla C^*) \quad (2)$$

where, N^* is the number density, r^* is the characteristic radius of the inclusions, D_{eff} is the effective diameter, C^* is the boundary flow of the concentration, S_{N^*} is the reduction in the number density caused by inclusion collision agglomeration.

2 Models and boundary conditions

The numerical model is based on the 170 t RH refining equipment with the parameters listed in Table 1. The bottom center of the ladle is set as the coordinate origin. A turbulence model was used to calculate the turbulent kinetic energy, while a discrete phase model (DPM) model was used to calculate the inclusion movement during the RH refining processes. The model considers gravity, buoyancy, Stokes forces and Brownian forces that act on the inclusions[12,13]. The inclusions were assumed to be spherical and had no influence on the flow field, and the volume of fluid (VOF) method was used to simulate the flow[6,8]. The interface tracking between the gas and liquid phases in the vacuum chamber was accomplished by solving the continuity equation for the volume fraction of each phase.

The mass flow rate of Ar as predetermined by the actual RH working conditions was limited to 70-180 m³/h. For the DPM model, the lower part of the vacuum chamber was set as the inlet boundary of the inclusions. Inclusions sized at 0.5-6 μm were primarily formed during the RH de-oxidation treatment. Experimental work[5] illustrated that 35.5% of the inclusions are in the range of 0.5-1 μm, 51% are 1-2 μm, 7.2% are 2-3 μm, and 6.3% are 3-6 μm. Based on the analysis results of real samples collected from RH processes, the total inclusion mass was calculated to be 0.21 kg in the 170 t molten steel.

Table 1 Dimensions of the RH system for modelling

Unit	Position	Value/mm
Ladle	Top diameter of ladle	3327
	Bottom diameter of ladle	2893
	Height of ladle	3185
RH	Diameter of vacuum chamber	1960
	Diameter of snorkels	520
	Nozzle diameter	6
	Height of vacuum chamber	3650

Table 2 Physical properties of liquid steel and inclusions

	Density /(kg/m³)	Viscosity /(kg/m·s)	Thermal conductivity /(W/m·K)	Specific heat capacity /(J/kg·K)
Liquid steel	7 000	0.0009	34	680
Al_2O_3 inclusion	4 000	-	1	600

The top of the vacuum chamber was set as the outlet. When the gas bubbles reach the boundary, they escape from the vacuum chamber at an inherent speed[6,14]. Non-slip boundary conditions were assumed for all wall surfaces, and the nodes of the near wall areas were treated with the scalable wall function.

The simulations assumed a liquid for the main fluid phase and argon for the secondary gas phase. Both the gas and liquid phases were assumed to be non-compressible, viscous, Newtonian fluids. Based on actual steel plant processing conditions, we used 133 Pa for the vacuum treatment at an operating temperature of 1 873 K. As the liquid surface of the vacuum chamber was assumed to be reflective, it does not have the ability to directly remove inclusions. The FLUENT software was used to calculate the flow field and inclusion growth through colliding and coarsening during the RH treatment. Table 2 lists the physical properties of the liquid steel and the inclusions used in the model calculations.

3 Simulation results

3.1 Effect of gas flow rate

Fig.1 shows the steady flow fields of RH system at Ar gas flow rates of 80, 120, 160, and 180 m³/h. The liquid steel flow rate in the up-leg snorkel increased with the greater Ar gas flow rates and reached a maximum at 160 m³/h before dropping off.

The contours of the turbulent kinetic energy and the turbulent dispersing rate in the vacuum chamber at the Z-X central section shows that the maximum turbulent kinetic energy is located at the upper part of up-leg snorkel near the liquid surface in the vacuum chamber (Fig.2(a)). The liquid steel, as accelerated by Ar bubbles, changed the flow direction at the liquid surface, resulting in a high level of turbulent kinetic energy. The turbulent kinetic dispersing rate is distributed in a similar pattern (Fig.2(b)). Both the turbulent kinetic energy and the turbulent dispersing rate gradually increased with higher gas flow rates and reached a maximum at an Ar flow rate of 160 m³/h before decreasing. The turbulent dispersing rate, ε, significantly influences the mixing time, t_m, during RH treatment, as given by $t_m \propto 1/\varepsilon^{1/3}$; therefore, a minimum mixing time was achieved at a gas blowing rate of 160 m³/h.

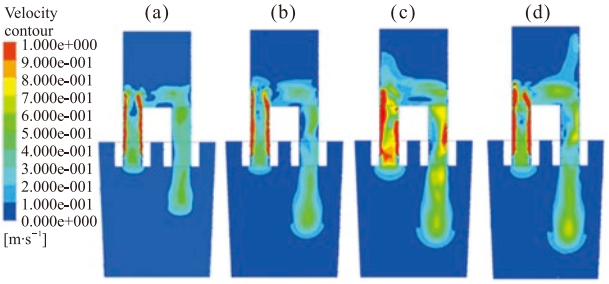

Fig.1 Velocity contours of flow field at Ar gas flow rates of (a) 80 m³/h, (b) 120 m³/h, (c) 160 m³/h, and (d) 180 m³/h

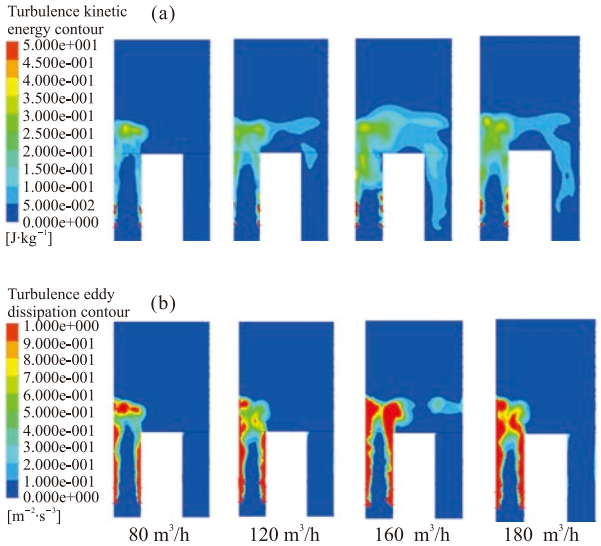

Fig.2 (a) Turbulent kinetic energy contours; (b) Turbulent Eddy dispersing contours; as different gas flow rates

Shear stress calculations for the up-leg snorkel indicate that the wall shear stress increases significantly with higher Ar gas flows, in particular, the throat area could be subjected to a 5 Pa or higher shear stress. Therefore, any further increase in the gas flow rate beyond 160 m³/h has relatively little impact on the liquid steel circulation but increases the wear of the lining and leads to splashing of the liquid steel in the vacuum chamber.

To verify the validity of the mathematical model used to simulate the liquid steel flow and inclusion movement in RH treatments, the velocity vector field at stable circulation conditions was compared with reported water model results[8]. As shown in Fig.3, the liquid steel enters the ladle from the down-leg snorkel and directly flows towards the bottom of the ladle before moving along the ladle bottom. The majority of the liquid steel subsequently flows back into the vacuum chamber through the up-leg snorkel, while the remaining steel forms a vortex near the descending stream. The calculated velocity vector diagram is in good agreement with the flow field distribution as measured using particle image velocimetry[8]. In addition, the simulated results indicate a 73.6% removal rate of small inclusions, which is consistent with the actual removal rate of 77.3% as measured in a previous study[5].

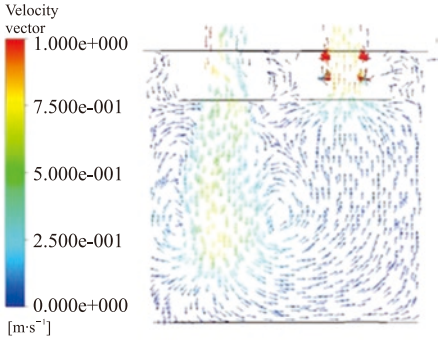

Fig.3 Calculated velocity vector field along central cross-section

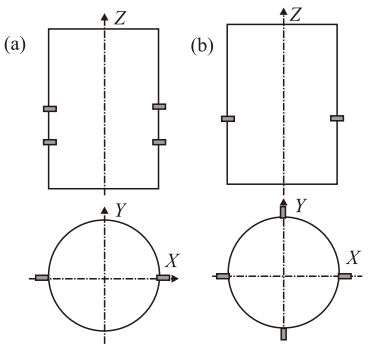

Fig.4 Schematic diagrams showing Ar nozzle positions in up-leg snorkel: (a) Original two-row design; (b) Proposed ingle-row design

3.2 Effect of Ar nozzle design

The effect of Ar nozzles on the removal efficiency of submicron inclusions was investigated in terms of the nozzle position and size. Based on the results discussed above, a constant gas flow of 160 m³/h was

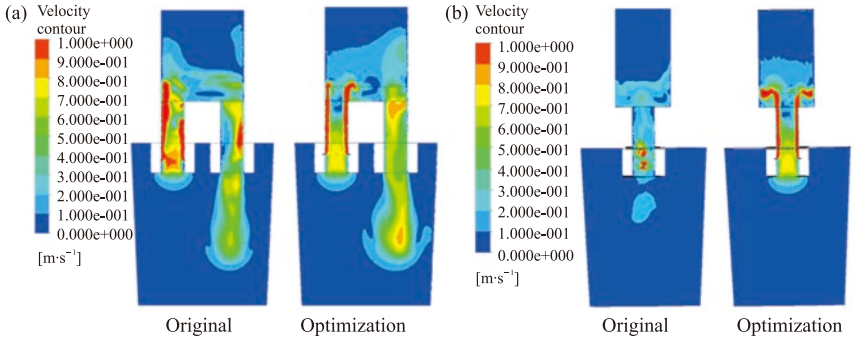

Fig.5 Comparison of flow field velocity contours before and after nozzle change: (a) *Z*-*X* cross section; (b) *Y*-*Z* (*X*=−675) cross section

used in the simulations. The original two-row Ar nozzle design with an inner diameter of 6 mm is compared with a proposed design consisting of single-row of Ar nozzles with a 3 mm nozzle diameter (see Fig. 4). The reduced Ar nozzle inner diameter resulted in smaller bubble sizes that improved the removal efficiency of submicron inclusions.

Flow field velocity contours revealed that the Ar gas flow is relatively uniform in the proposed nozzle arrangement and generates a much higher up-lifting force for the liquid steel circulation. Therefore, the proposed Ar nozzle design improves the removal efficiency of inclusions (see Fig.5).

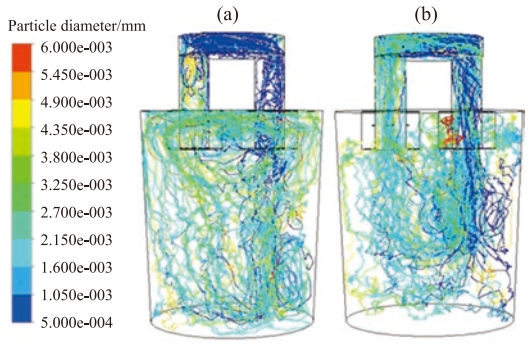

Fig.6 Movement of different sized inclusions: (a) Before Ar nozzle change; (b) After Ar nozzle change

The turbulent kinetic energy and turbulent dispersing rate in the degasser chamber increased significantly after the proposed nozzle change, particularly at the *Y*-*Z* (*X* = −675) plane. Therefore, the new nozzle reduces the mixing time. Inclusion particle trajectories show a similar flow pattern as the liquid steel flow field, as illustrated in Fig.6. However, there is a high degree of oscillation in the particle mixing movement due to the strong influence of Brownian motion for the submicron inclusions[11,12]. The random Brownian motion causes instantaneous velocity differences between the particles and the liquid steel flow field. The movement of small inclusions is predominately influenced by the liquid steel flow and Brownian motion.

In the proposed nozzle design, there are relatively few trajectory lines for submicron inclusions in the vacuum chamber; however, the trajectories of the 2-3 μm inclusions increased. This indicates an increased collision and coarsening of the submicron inclusions after the design change. In addition, there are relatively few inclusion trajectories below the free surface of the steel ladle after the proposed nozzle change. In contrast, the original design had several inclusions with trajectories that were immediately below the free surface of the steel ladle, which were most likely carried away by the liquid steel and remained in the circulation. The model simulations revealed that the new Ar nozzle improves the removal rate of inclusions from the original 73.6% to 87.5%. As a result, the improved Ar nozzle design in RH refining positively impacts the magnetic properties of non-oriented silicon steel.

4 Discussion

Our previous work[5] showed that conventional Ar nozzles in RH refining processes are less effective at removing submicron inclusions in non-oriented silicon steel than the proposed design. As submicron inclusions (0.5-1 μm) have a significant detrimental effect on the magnetic properties of non-oriented silicon steel, it is critical to improve their removal efficiency during the RH refining process. A proposed change in the Ar nozzle arrangement in combination with the reduced nozzle inner diameter previously demonstrated the significant improvement in the submicron inclusions removal.

Fig.7 shows the removal process for submicron inclusions as a function of the treatment time in the original and modified Ar nozzle design. The density of the submicron inclusions is high at the beginning of the RH treatment (*t* = 100 s); therefore, inclusion

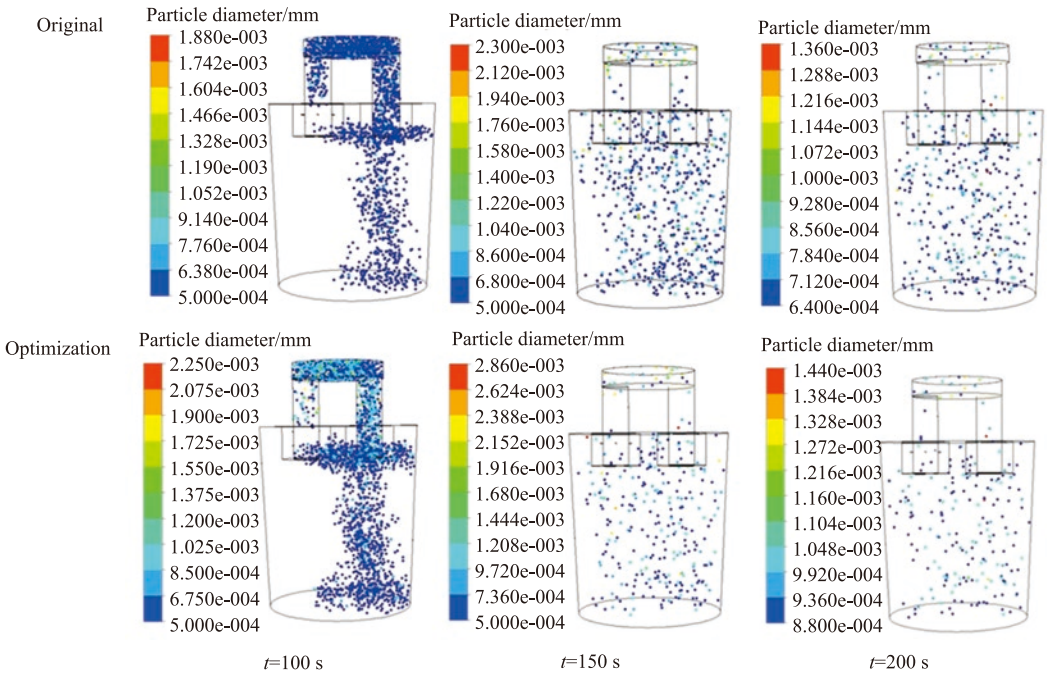

Fig.7 Removal process of submicron inclusions with treatment time before and after Ar nozzle design change

collisions are more likely to occur. The inclusions after colliding and coarsening reach the vicinity of the ladle bottom with the descending steel stream before moving upwards to reach the ladle free surface where the inclusions are trapped and removed with the top slag. As the RH treatment progresses, the probability of collisions between inclusions is reduced due to the dramatic reduction in their density. After 200 s, the cleanliness of the liquid steel was further improved as the large-sized inclusions were substantially removed, and the majority of the remaining inclusions were between 0.5 and 1.5 μm.

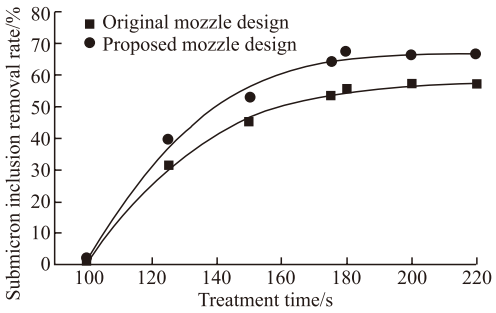

Fig.8 Comparing the removal rate of submicron inclusions with treatment time before and after Ar nozzle change

In order to understand the submicron inclusion removal in RH system during vacuum process, the term of the removal rate of submicron inclusions is defined. And the removal rate of submicron inclusions is the ratio of the removal number of submicron inclusions, *i e*, the difference between the number of submicron inclusions at any time during the vacuum process and the total number of submicron inclusions originally in the liquid steel before the process, to the total number of submicron inclusions before the vacuum treatment.

Fig.8 compares the removal rates for submicron inclusions before and after the Ar nozzle design change. The removal rates for submicron inclusions in both designs followed similar trends. That is, there was a rapid increase within the first 2 min followed by a gradual increase before leveling off after 3 min. The proposed change in the Ar nozzle design results in a significant increase in the removal efficiency of submicron inclusions, which reduces the iron loss and improves the magnetic properties of non-oriented silicon steel.

5 Conclusions

The effects of optimized Ar nozzles on the removal rate of submicron inclusions during the RH refining process was investigated via mathematical modelling to improve the magnetic properties of non-oriented silicon steel. The main conclusions are summarized as follows.

a) Increasing the up-lifting gas flow rate is favorable for inclusion removal because of the increased liquid steel velocity, turbulent energy and turbulent dispersing rate. However, when the gas flow rate is higher than 160 m³/h, the effects on the flow velocity of the liquid steel are relatively small, while the erosion of the refractory lining increases dramatically, especially around the throat area.

b) A new Ar nozzle design for an RH degasser

was proposed and numerically evaluated to increase the removal rate of inclusions from 73.6% to 87.5%. The four nozzles were positioned equally in a single row to replace the original four nozzles sitting on oppose sides in two rows. The inner diameter of the gas nozzles was reduced from the original 6 mm to 3 mm. The model calculations showed that the proposed design delivers a more uniform gas flow for the up-lifting action and increased the liquid steel velocity at the down-leg snorkel. In addition, the new design increased the turbulent energy and turbulent dispersing rate of liquid steel, which resulted in a shorter mixing time.

c) The model simulations indicated that the new nozzle design for the RH degasser improved the collision and coarsening of submicron inclusions (0.5-1 μm), which was primarily due to the increased turbulent kinetic energy and turbulent dispersing rate. As a result, the removal rate of submicron inclusions increased significantly from 57.1% in the original design to 66.4% in the new design. The proposed new Ar nozzle design improves the magnetic properties of non-oriented silicon steel by increasing the removal efficiency of submicron inclusions.

References

[1] Du LY, Zhou GF, Liu J, *et al.* Fatigue Cracking Characterization of High Grade Non-oriented Electrical Steels[J]. *J. Wuhan Univ. Technol.-Mater. Sci. Ed.*, 2017, 32(6): 1 329-1 335

[2] Bóc I, Cziráki Á, Gróf T, *et al*. Analysis of Inclusions in Cold-rolled No Si-Fe Strips[J]. *J. Magn. Magn. Mater*., 2015, 83(1): 381-383

[3] Hawezy D. The Influence of Silicon Content on Physical Properties of Non-oriented Silicon Steel[J]. *J. Mater. Sci. Technol.*, 2017, 33(2): 1-10

[4] Wan Y, Chen W. Effect of Boron Content on the Microstructure and Magnetic Properties of Non-oriented Electrical Steels[J]. *J. Wuhan Univ. Technol. -Mater. Sci. Ed.*, 2015, 30(3): 574-579

[5] Chen TY, Liu J, Cheng ZY, *et al.* Study on Inclusion Behavior in RH Refining Process of Non-oriented Silicon Steel[J]. *Journal of Wuhan University of Science and Technology*, 2019 (1): 1-7 (in Chinese)

[6] Kuwabara T, Umezawa K, Mori K, *et al.* Investigation of Decarburization Behavior in RH-reactor and Its Operation Improvement[J]. *Transactions of the Iron and Steel Institute of Japan*, 1988, 28(4): 305-314

[7] Zhu MY, Huang ZZ. Simulation Study on RH Vacuum Decarburization Refining Process[J]. *Acta Metall. Sinica*, 2001, 37(1): 91-94(in Chinese)

[8] Ling HT, Guo C, Conejo AN, *et al*. Effect of Snorkel Shape and Number of Nozzles on Mixing Phenomena in the RH Process by Physical Modeling[J]. *Metall. Res. Technol*., 2017, 114(1): 111

[9] Ling HT, Li F, Zhang L, *et al*. Investigation on the Effect of Nozzle Number on the Recirculation Rate and Mixing Time in the RH Process using VOF+ DPM Model[J]. *Metall. Mater. Trans. B*, 2016, 47(3): 1 950-1 961

[10] Yan W. Numerical Study on the Effect of Argon Blowing on the Flow of RH Vacuum Refining Cycle[D]. *Northeastern University*, 2012 (in Chinese)

[11] Ai XG, Wang CS, Meng FT, *et al*. Numerical Simulation of the Movement and Removal of Inclusions in Al_2O_3 during RH Refining Process[J]. *Journal of Iron and Steel Research*, 2016, 28(1): 20-24. (In Chinese)

[12] Wang Y, Li H, Guo LF. Numerical Simulation of Force of Spherical Inclusion Particles in Liquid Steel[J]. *Journal of University of Science and Technology Beijing*, 2013, 35(11): 1 437-1 442(in Chinese)

[13] Treadgold CJ. Behaviour of Inclusions in RH Vacuum Degasser[J]. *Ironmak. Steelmak.*, 2003, 30(2): 120-124

[14] Xu J, Huang F, Wang X, *et al.* Investigation on the Removal Efficiency of Inclusions in Al-killed Liquid Steel in Different Refining Processes[J]. *Ironmak. Steelmak*., 2017, 44(6): 455-460